Depth profile of the implantation-enhanced intermixing of Ga^+ focused ion beam in AlAs/GaAs quantum wells

Soheyla Eshlaghi[a)]
Universität Dortmund, Experimentalphysik III, Otto Hahn Strasse 4, D-44221 Dortmund, Germany, and Ruhr-Universität Bochum, Angewandte Festkörperphysik, Universitätstrasse 150, D-44780 Bochum, Germany

C. Meier
Ruhr-Universität Bochum, Angewandte Festkörperphysik, Universitätstrasse 150, D-44780 Bochum, Germany

Dieter Suter
Universität Dortmund, Experimentalphysik III, Otto Hahn Strasse 4, D-44221 Dortmund, Germany

D. Reuter and A. D. Wieck
Ruhr-Universität Bochum, Angewandte Festkörperphysik, Universitätstrasse 150, D-44780 Bochum, Germany

(Received 21 June 1999; accepted for publication 25 August 1999)

The implantation-induced intermixing depth profile for 100 keV Ga^+ ions was determined by photoluminescence measurements on a series of samples containing quantum wells at variable depth from the surface but identical thickness. They were uniformly implanted and subsequently a rapid thermal annealing was applied. The measured maximum of the intermixing occurred at a depth of about 70 nm, significantly deeper than theoretical predictions. These results are important for achieving sufficient intermixing with a low implantation dose, thereby optimizing crystal quality and lateral resolution. © *1999 American Institute of Physics.* [S0021-8979(99)00323-0]

Focused ion beam (FIB) implantation is an attractive method to fabricate optical devices such as quantum wires, quantum dots,[1–3] distributed Bragg reflectors,[4] and distributed feedback lasers[5] by lateral structuring of proper samples. After implantation and rapid thermal annealing (RTA) implantation enhanced intermixing takes place, resulting in a modification of the band gap and refractive index in the implanted areas. The most common ion source used for implantation is Ga^+, because it is the most stable liquid metal ion source for FIB.[6] Its nuclear efficiency with respect to the collisional mechanism also adds to its attractiveness.[7] Furthermore, Suzuki *et al.*[8] have shown that the implantation defects can be annihilated almost perfectly in Ga^+ ion-implanted GaAs/AlAs materials, where the implanted ions are also constituents.

The degree of intermixing depends for a given ion energy on the implantation dose and RTA conditions as well as on the depth of the structure. The higher the implantation dose, the higher is the intermixing effect.[9] Unfortunately, the implantation damage reduces the crystal and thereby the optical quality. The intermixing also increases with increasing annealing temperature and duration. However, the effect is limited by saturation of the defects[10] and eventually by unwanted intrinsic intermixing in unimplanted areas. The third parameter for a defined compositional intermixing is the depth of the structure which is to be modified by FIB.

For an implantation direction normal to the sample surface large deviations from the theoretically predicted ion range have been reported.[11–14] This deviation is believed to be due to the channeling mechanism that is neglected in the Monte Carlo code TRIM.[15] Laruelle *et al.*[14] have shown that the focused ion beam penetrates in GaAs/Al_xGa_{1-x}AsQW structures much deeper than theoretically predicted for amorphous GaAs (TRIM). They also found a smaller lateral straggling than predicted theoretically, resulting in a higher lateral resolution. According to their interpretation both effects are due to channeling. However, it is not yet well studied, whether and how the channeling affects the ion depth distribution. Implantation at normal incidence not only improves the lateral resolution by reducing straggling, but also maintains this resolution over the whole sample surface. For tilted implantation, dynamic focus control must be used.[16]

Low dose implantation provides several advantages. The implantation damage remains small, the dose can be kept below the amorphization dose, and the resulting structures have better crystal quality. For maskless implantation with high lateral resolution it is also important to keep the total dose small to avoid the unwanted side dose implantation in nominally nonimplanted region. This side dose could accumulate about 10^{13} ions/cm^2 in nonimplanted regions for quantum wires implanted with a dose of 5×10^{14} ions/cm^{-2} and a line spacing of 100 nm.[6] Furthermore, a higher implantation dose requires a longer implantation time, thus increasing the probability of fluctuations in the ion current and the ion focus, which may result in inhomogeneous geometry and potential. For instance in some cases the quantum wire energy states could not be resolved in the photoluminescence (PL) spectrum.[2]

[a)]Electronic mail: soheyla@fuj.physik.uni-dortmund.de

In order to determine the depth for which the maximum intermixing occurs, we grew several samples on (100)-oriented GaAs substrates by molecular beam epitaxy (MBE). The growth conditions were kept constant for all samples. Each sample consists of quantum wells (QWs) with the same thickness but various depths from the surface. One advantage of using QWs with the same thickness is that one is able to determine the intermixing depth profile experimentally, without relying on theoretical calculations of the interdiffusion length for intermixed QWs,[10] which are usually based on an error function potential model. Each sample includes two QWs (5.2 and 13.7 nm) located in depths ranging from 15 to 300 nm below the surface. The barriers are AlAs/GaAs superlattices with a period of 2.7 nm. This kind of barriers was chosen rather than $Al_xGa_{1-x}As$ barriers because they are more resistant against implantation damage[17] and because a pure AlAs layer at the boundary of the QW offers more Al for the interdiffusion in GaAs QW than $Al_xGa_{1-x}As$ layers.

For all samples, the implantation dose was about 7×10^{12} ions/cm^2 and the beam current was kept constant at 20 pA to exclude the influence of the beam current on the intermixing. Areas of 1 mm×1 mm were implanted uniformly on each sample. The ion beam diameter was about 100 nm. After implantation the samples were annealed at 750 °C for 20 s. Measurements in nonimplanted areas verified that under these RTA conditions no intrinsic interdiffusion occurs in nonimplanted areas and the measured energy shift reflects therefore, alone the concentration profile of the implantation induced point defects, e.g., vacancies and interstitials. For higher annealing temperatures, which are required for higher implantation doses, intrinsic interdiffusion could also take place, complicating the interpretation of the measured energy shift. The effect of the implantation enhanced intermixing was characterized by PL measurements at a temperature of 4 K with a laser diode ($\lambda=682$ nm) as an excitation source. The excitation laser power and beam diameter were 0.5 mW and 175 μm, respectively.

The measured depth dependence of the energy shift due to the intermixing is shown in Fig. 1 for two different QW widths of 5.5 and 13.7 nm. The energy shift between the PL peaks in implanted and nonimplanted areas of each QW served as a measure of intermixing (inset in Fig. 1). For 5.5 nm QWs the energy shift increases first rapidly with depth and reaches a maximum at a depth of about 70 nm. Beyond this depth it slowly decreases and at a depth of 260 nm there are still sufficient defects to induce a significantly energy shift of 10 meV. The error bars in Fig. 1 give the standard deviation determined from PL measurements for one of the samples (with 5.5 nm QW at a depth of 60 and 13.7 nm at 95 nm) which was implanted and annealed several times. In contrast, the depth profile of the 13.7 nm QWs indicates no clear maximum. The reason for this behavior is that for the thicker QWs the same interdiffusion length causes a smaller shift in the luminescence energy, which is of the same order as the experimental errors. It is interesting that the 13.7 nm QW shows an energy shift of about 1.5 meV for a depth of 300 nm which indicates the existence of a relatively large number of implantation defects even in this regime.

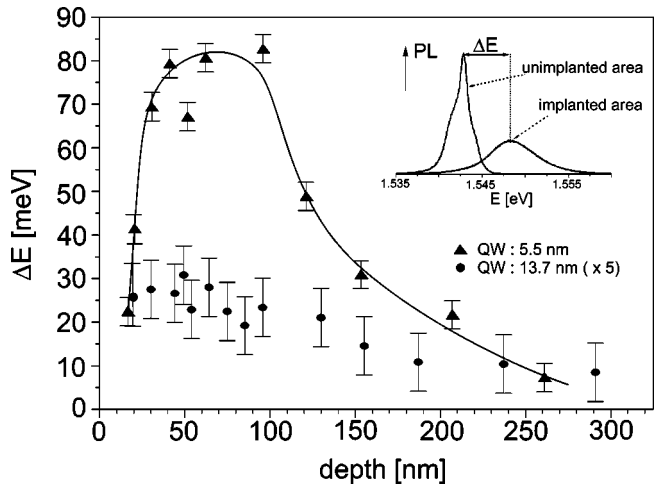

FIG. 1. Intermixing depth profile for 100 keV Ga^+ ions in GaAs/AlAs QWs of two different thicknesses: 5.5 nm (triangles) and 13.7 nm (circles). Note the different scaling of the two data sets.

The measured energy shift ΔE corresponds to a change of the QW thickness and consequently to an interdiffusion length. Using a simple error function potential model for interdiffused QWs[10] we calculated the interdiffusion length as a function of the depth as shown in Fig. 2. Large interdiffusion lengths are achieved for this relatively low ion dose and moderate RTA condition. The maximum interdiffusion length[18] is about 1.3 nm at a depth at 70 nm. This corresponds to an interdiffusion constant of 1.1×10^{-17} cm^2/s.

According to TRIM[19] the maximum of the vacancies and ion profile are at a depth of about 28 and 44 nm, respectively. We assume that the implantation induced vacancies and interstitials are predominantly responsible for the intermixing in this implantation dose regime.[10] The presence of the vacancies[20] and the existence of the Al and Ga concentration gradient at the QW interface cause an interdiffusion current during RTA and promote the intermixing. It appears likely that the deviation between the experimentally measured depth of maximum and the theoretically predicted value is due to the channeling effect, which is neglected in TRIM calculations. For implantation doses higher than the

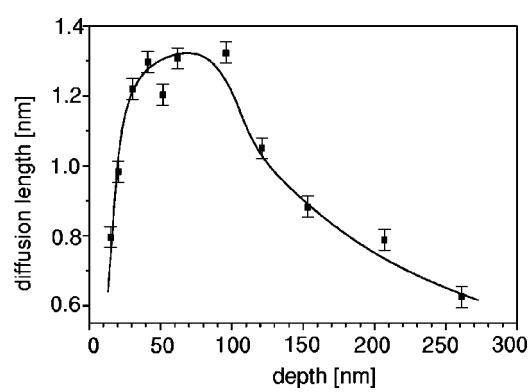

FIG. 2. Calculated interdiffusion length as a function of depth for 5.5 nm QW implanted with a dose of 7×10^{12} ions/cm^2 and annealed at 750 °C for 20 s.

amorphization dose additional collisional intermixing occurs,[9] and an amorphous layer is created. This slightly reduces the effective channeling distance.[21]

In conclusion, we have determined the depth profile of the implantation enhanced intermixing for 100 keV Ga^+ions. The maximum of the profile is at a depth of about 70 nm and thus 40 nm deeper than theoretically predicted. To avoid any dependence of these results on theoretical models we measured the photoluminescence wavelength of a series of samples with identical QWs at different depths. This approach also resulted in relatively small experimental errors that were independent of depth. Further investigations are required to determine the mechanisms, which are responsible for the intermixing. In particular it would be interesting to investigate whether the depth profile of the vacancies (or ions) is the same as the depth profile for the intermixing and whether it is the channeling which causes the deviation between experimentally determined intermixing depth and the theoretically predicted one.

This work is supported by Graduiertenkolleg 50 of the Deutsche Forschungsgemeinschaft. One of us (D.R.) would like to thank GK 384 of the Deutsche Forschungsgemeinschaft for financial support. The authors are indebted to I. Kamphausen for support within a MBE-Project of the Ministerium für Schule und Weiterbildung, Wissenschaft und Forschung des Landes Nordrhein-Westfalen.

[1] F. E. Prins, G. Lehr, M. Burkard, J. Cibert, H. Schweizer, and M. H. Pilkuhn, Appl. Phys. Lett. **62**, 1365 (1993).
[2] Y. Hirayama, S. Tarucha, Y. Suzuki, and H. Okamoto, Phys. Rev. B **37**, 2774 (1988).
[3] C. Vieu, M. Schneider, G. Benassayag, R. Planel, L. Biriotheau, J. Y. Marzin, and B. Descouts, J. Appl. Phys. **71**, 5012 (1992).
[4] A. J. Steckl, P. Chen, X. Cao, H. E. Jackson, M. Kumar, and J. T. Boyd, Appl. Phys. Lett. **67**, 179 (1995).
[5] K. Ishida, E. Miyachi, T. Morita, T. Takamori, T. Fukunaga, H. Hashimoto, and H. Nakashima, Jpn. J. Appl. Phys., Part 2 **26**, L285 (1987).
[6] Y. Hirayama, Y. Suzuki, and H. Okamoto, Surf. Sci. **178**, 98 (1986).
[7] C. Vieu, M. Schneider, R. Planel, H. Launois, B. Descouts, and Y. Gao, J. Appl. Phys. **70**, 1433 (1991).
[8] Y. Suzuki, Y. Hirayama, and H. Okamoto, Jpn. J. Appl. Phys., Part 2 **25**, L912 (1986).
[9] Y. Hirayama, Jpn. J. Appl. Phys., Part 1 **28**, 162 (1989).
[10] J. Cibert, P. M. Petroff, D. J. Werder, S. J. Pearton, A. C. Gossard, and J. H. English, Appl. Phys. Lett. **49**, 223 (1986).
[11] F. Laruelle, P. Hu, R. Simes, R. Kubena, W. Robinson, J. Merz, and P. M. Petroff, J. Vac. Sci. Technol. B **7**, 2034 (1989).
[12] L. R. Harriot, H. Temkin, R. A. Hamm, J. Weiner, and M. B. Parish, J. Vac. Sci. Technol. B **7**, 1467 (1989).
[13] R. Germann, A. Forchel, M. Bresch, and H. P. Meier, J. Vac. Sci. Technol. B **7**, 1475 (1989).
[14] F. Laruelle, A. Bagchi, M. Tsuchiya, J. Merz, and P. M. Petroff, Appl. Phys. Lett. **56**, 1561 (1990).
[15] J. F. Ziegler, Manual, IBM Research, Yorktown, New York, 1991.
[16] L. Bischoff, J. Teichert, and E. Hesse, Microelectron. Eng. **27**, 351 (1995).
[17] A. G. Cullis, P. W. Smith, D. C. Jacobsen, and J. M. Poate, J. Appl. Phys. **69**, 1279 (1991).
[18] Interdiffusion length is defined as $\sqrt{D\times t}$, where D is the diffusion constant and t is the annealing time.
[19] We used TRIM 98.1 and SRIM 2000 codes.
[20] W. P. Gillin, D. J. Dunstan, K. P. Homewood, L. K. Howard, and B. J. Sealy, J. Appl. Phys. **73**, 3782 (1992).
[21] R. Kalish, L. Y. Kramer, K. K. Law, J. L. Merz, L. C. Feldman, D. C. Jacobson, and B. E. Weir, Appl. Phys. Lett. **61**, 2589 (1992).